AGNAGN seminar
chapter 8. Infrared Radiation and Molecules
8.1-8.4

Taiki Kikuchi

July 25

8.1 Introduction

2 types of fronts.

- **Matter-bounded** : The outer boundary occurs at the outer edge of the gas.
- **Radiation-bounded** : Ionization front defines the outer boundary (which is seen in visible light).

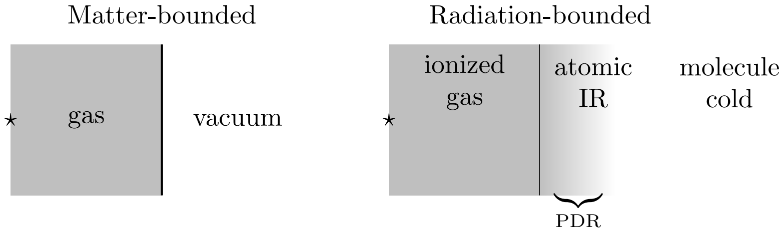

Matter-bounded

⋆ gas

vacuum

Radiation-bounded

⋆ ionized gas

atomic IR

molecule cold

PDR

- **PDR (photodissociation region)** : Molecules are dissociated by photons with energy less than $h\nu_0$.
- From PDR, the **far-infrared** fine-structure lines ([OI]$\lambda 63\mu$m, [CII]$\lambda 158\mu$m) are emitted.

8.2 Entire radiation

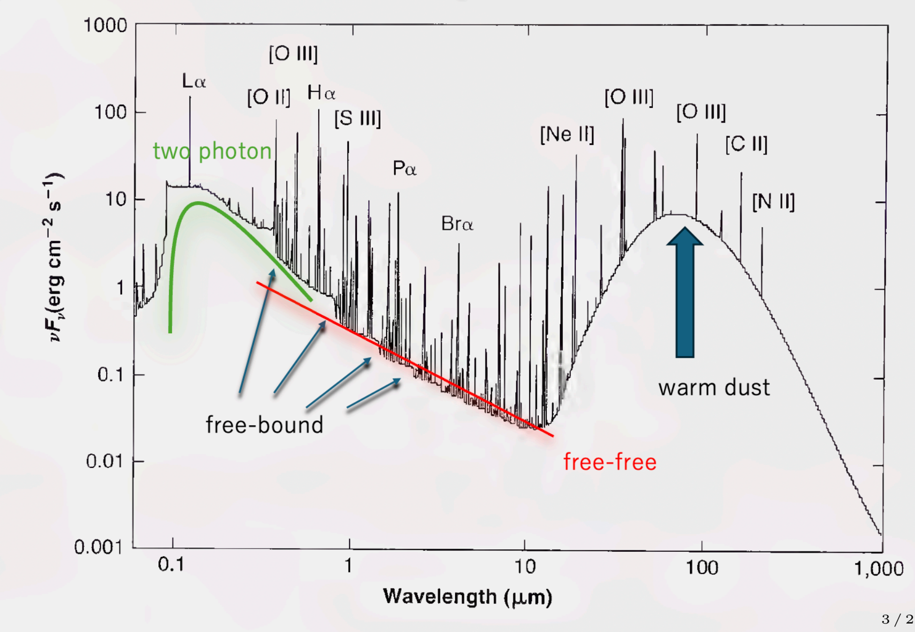

8.2 The radiation field striking the PDR

How much energy is injected into the PDR ?

- LyC($Q(\mathrm{H}^0)$) is **largely absorbed** inside the HII region.
- Balmer continuum($[6.0, 13.6]$eV) plays an important role.
- The ratio of the radiation field striking the PDR is

$$G_0 = \int_{6\mathrm{eV}}^{13.6\mathrm{eV}} \frac{4\pi J_\nu d\nu}{1.6\times10^{-3}\mathrm{erg\,s^{-1}\,cm^{-2}}} \tag{1}$$

  , where the denominator $1.6\times10^{-3}\mathrm{erg\,s^{-1}\,cm^{-2}}$ is the **mean galactic radiation field**. Note that this physical quantity G_0 is **dimensionless**.
- In inner regions of the Orion nebula $G_0 \sim 4\times10^5$.

8.2 Ionization and temperature structures

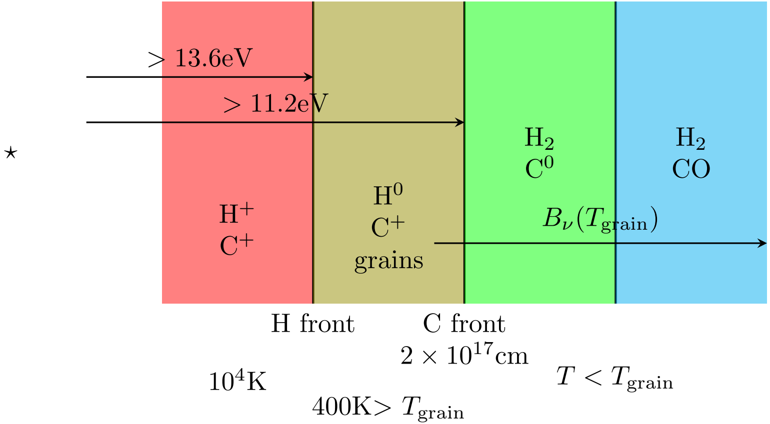

8.2 Ionization and temperature structures

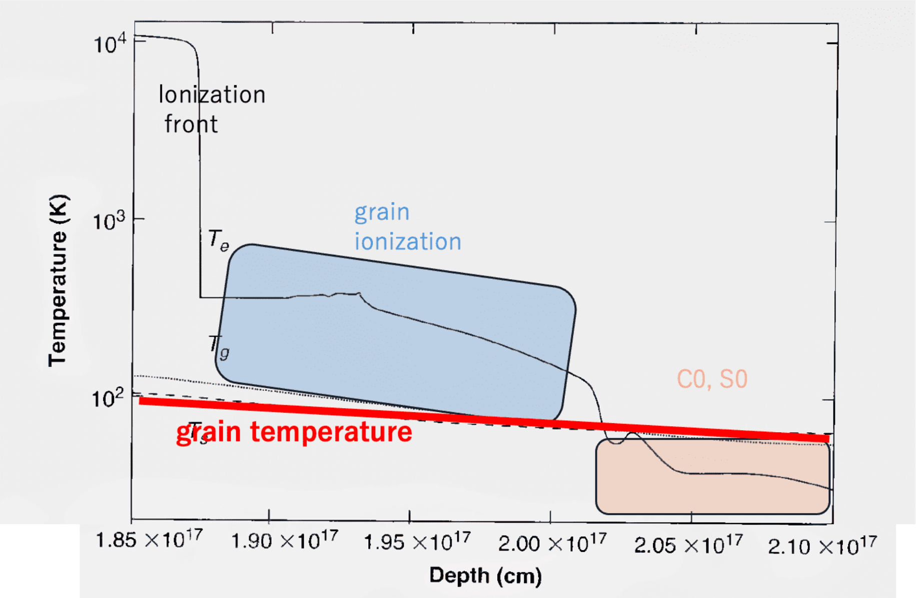

8.2 Ionization and temperature structures

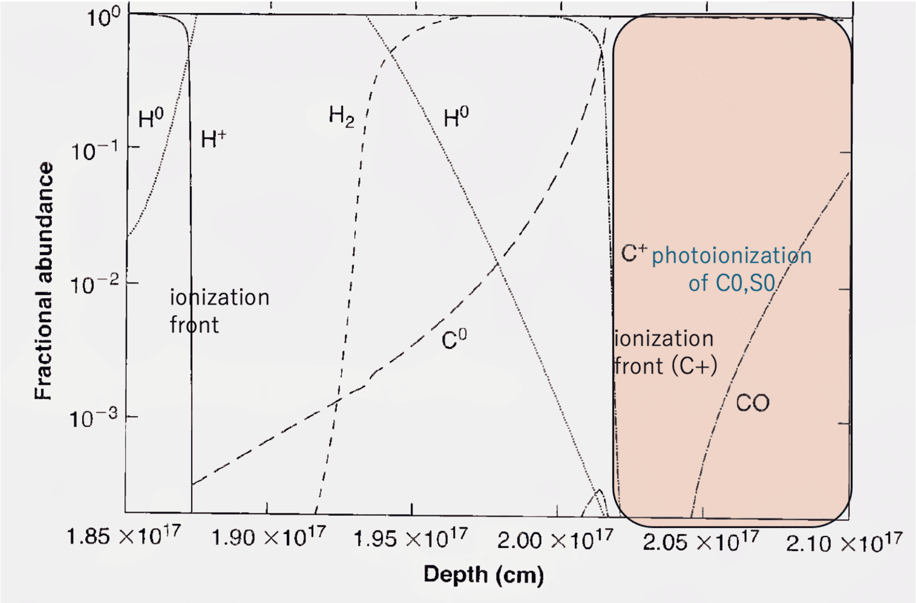

8.3 QM of H_2 molecule

Hamiltonian of H_2 molecule

$$\hat{H} = \hat{H}_{\text{electron}} + \hat{H}_{\text{vib}} + \hat{H}_{\text{rot}} + \hat{H}_{\text{spin}} \tag{2}$$

where $\hat{H}_{\text{electron}}$ is the Hamiltonian of the electron (Born–Oppenheimer approximation), and $\hat{H}_{\text{vib}} := \frac{1}{2}\mu\omega^2\hat{q}^2$, $\hat{H}_{\text{rot}} = \frac{\hbar^2 \hat{J}(\hat{J}+1)}{2\mu r^2}$.

Note that $\hat{H}_{\text{spin}}$ is the spin Hamiltonian of protons (not electrons).

Its eigen state

$$|\Psi\rangle = |n, l, m\rangle \otimes |\nu, J\rangle \otimes |T; T_z\rangle \tag{3}$$

where T is coupled spin number.

Possible spin state $|T; T_z\rangle$

$$\text{triplet} \begin{cases} |1;1\rangle = |\uparrow\rangle \otimes |\uparrow\rangle \\ |1;0\rangle = \frac{1}{\sqrt{2}}(|\uparrow\rangle|\downarrow\rangle + |\downarrow\rangle|\uparrow\rangle) \\ |1;-1\rangle = |\downarrow\rangle \otimes |\downarrow\rangle \end{cases} \tag{4}$$

$$\text{singlet} \begin{cases} |0;0\rangle = \frac{1}{\sqrt{2}}(|\uparrow\rangle \otimes |\downarrow\rangle - |\downarrow\rangle \otimes |\uparrow\rangle) \end{cases} \tag{5}$$

8.3 Antisymmetry

Since 2 protons are Fermion, the overall wavefunction must be antisymmetric.

$$\text{triplet : symmetric} \quad \rightarrow \quad \text{odd } J(\text{ortho;antisymmetric}) \tag{6}$$

$$\text{singlet : antisymmetric} \quad \rightarrow \quad \text{even } J(\text{para;symmetric}) \tag{7}$$

when the electrons are in the ground state($X^1\Sigma$).
Following selection rule

- J can only change by 0 or by 2 through the transitions which occur by quadrupole radiation(H_2 doesn't have dipole moment).

At fixed temperature, the statistical weight of an ortho-H_2 rotational level is $3(2J+1)$ and that of an para-H_2 is $2J+1$.
Typical values

- Typical transition probabilities for “ forbidden ” electrical-quadrupole rovibrational transitions are $A \simeq 10^{-6\sim-7}\mathrm{s}^{-1}$.
- Typical collision rate coefficients are $\simeq 10^{-12\sim-11}\mathrm{cm}^3\,\mathrm{s}^{-1}$.
- The resulting $n_{\mathrm{crit}} \simeq 10^{3\sim5}\mathrm{cm}^{-3}$. Below this density, collisional excited H_2 largely decays with a photon.

8.3 Rovibrational energy levels of H_2

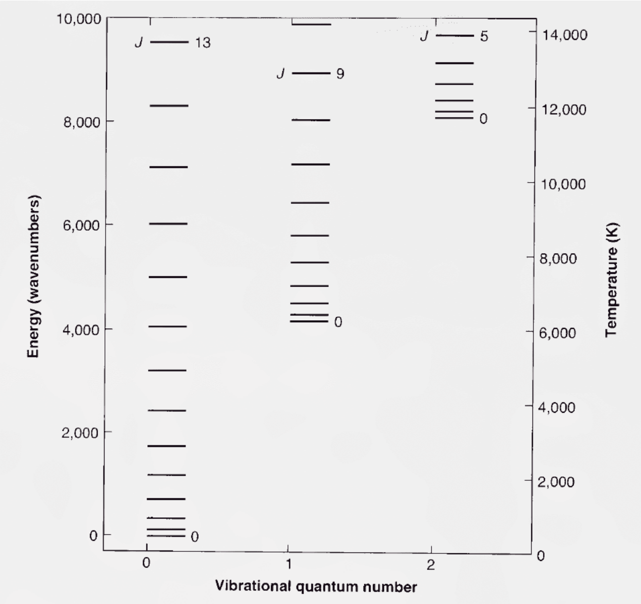

8.3 Rovibrational energy levels of H_2

Despite the great abundance of H_2, its lines are faint and hard to detect. Reason for this

- Eigen value of the rotational Hamiltonian is $E_J = \frac{\hbar^2 J(J+1)}{2\mu}$.
- μ is very small and this results in too high ΔE_J to excite.
- The lowest quadrupole transition ($\nu = 0 \to 0, J = 2 \to 0$) requires $\lambda 28.2 \mu\text{m}, 500\text{K}$, which is difficult to observe from the ground.
- Lines with observable wavelength arise from transitions with $\nu = 2 \to 0, J \geq 10$ which have far higher excitation temperature.
- Typical temperature in PDR is lower than 500K.

As a result there are very few collisionally excited H_2 lines emitted from within a PDR.

8.3 Formation of H_2

H_2 is hard to form naturally because

- In a two H atoms collision, energy and angular momentum should be conserved, which doesn't allow two H atoms stay bounded.
- If in the dense environment, three-body process can form H_2 (a third particle acts as a catalyst).
- In many ISM environment, the density is low and its rate is negligible.

However, when the ISM contains grains,

- H_2 is mainly formed by catalysis on grain surfaces.
- The formation energy is absorbed into the solid grain.
- The formation rate is

$$R = 0.5 n(\mathrm{H}^0) n_d \pi a^2 \bar{u} S(T) \mathrm{cm}^{-3}\,\mathrm{s}^{-1} \tag{8}$$

where n_d: dust density, πa^2: cross section, $S(T)$:the probability that an atom will stick, $\bar{u}$:the mean velocity.

8.3 Formation of H_2

In practice, some assumptions are adopted

- The dust to gas ratio is assumed to be constant.

$$n_d \pi a^2 = k n_{\mathrm{H}}, \quad k = \mathrm{const.} \tag{9}$$

  where $n_{\mathrm{H}} \simeq n(\mathrm{H}^0) + n(\mathrm{H}^+) + 2n(\mathrm{H}_2)$.

Also we note that

- The binding energy of H_2 is 4.5eV, which is too large to dissociate by collision.
- The direct photoionization $\mathrm{H}_2 + \mathrm{h}\nu \rightarrow \mathrm{H}_2^+$ is inefficient($\because$ few photons are transmitted into PDR).
- Convertion of ortho-para type occurs when H_2 leave the grain surface in a variety of energy states.

8.3 Photodissociation of H_2 (Solomon process)

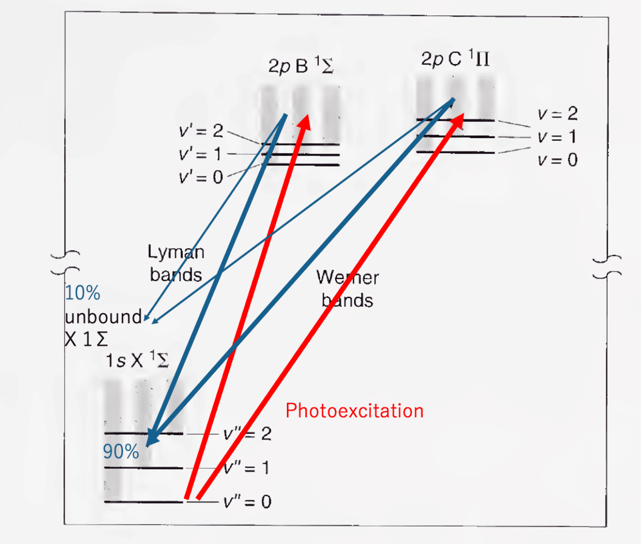

8.3 Photodissociation of H_2

The rate of this Solomon process is given as

$$R_{\rm pump} = 3.4 \times 10^{-10} \beta(\tau) G_0 \exp(-\tau_{\rm LW}) [{\rm s}^{-1}] \tag{10}$$

where G_0:energy injection by stellar continuum, $\tau_{\rm LW}$: optical depth of Lyman-Werner bands ($\sim 2.5 A_V$), $\beta(\tau)$: self-shielding effect.

$$\tau \simeq 1.2 \times 10^{-14} \frac{N({\rm H_2})}{u({\rm H_2})}, \quad N: \text{column density}, \quad u: \text{line width} \tag{11}$$

Therefore,

- $N(H_2) < 10^{14} {\rm cm}^{-2}$ → self-shielding is not effective, which results in high fraction of atomic H.
- $N(H_2) > 10^{14} {\rm cm}^{-2}$ → self-shielding is effective, and the gas is largely molecule.

8.3 Heating by H_2

- 90% of the photoexcited H_2 decay into some excited state with electron state $X^1\Sigma$.
- It results in overpopulation of the excited states

$$n_{\mathrm{exc}} > n_{\mathrm{gr}} \exp(-\Delta E/k_{\mathrm{B}}T) \tag{12}$$

- So, the heating of the gas by collisional deexcitation exceeds the cooling by radiation.
- In this process, the H_2 emission spectrum of a PDR is highly non-thermal.

8.4 Formation of CO

Direct reaction $C + O \rightarrow CO$ is possible but **unlikely** (small cross section).
→ ion-molecule reaction (induced by electric dipole)

- Most important first step is radiative association reaction

$$C^+ + H_2 \rightarrow CH_2^+ + h\nu \tag{13}$$

$$CH_2^+ + e^- \rightarrow CH + H \tag{14}$$

- Secondary, neutral exchange reaction is also important

$$CH + O \rightarrow CO + H \tag{15}$$

This is one of the reason CO forms at deeper regions in a PDR than H_2 (first reaction needs H_2).

8.4 CO energy levels

One big difference from H_2 is

- Energy eigen value $E_J = \dfrac{\hbar^2 J(J+1)}{2\mu}$.
- When CO, the moment of inertia μ is far larger → energy gap is much smaller.
- As a result CO is collisionally excited to much higher rotational levels in a PDR than is H_2.
- The transition probabilities $A_{ul} \sim 10^{-7\sim-5}\mathrm{s}^{-1}$ for $J \leq 5$.
- The corresponding critical densities are $10^{4\sim6}\mathrm{cm}^{-3}$.
- Under most circumstances, the lower J lines are optically thick since CO is abundant.

8.4 In practice

CO lines are more easily detected and measured thanks to the great sensitivity of radio receivers.
So, relation between CO lines and H_2 characteristics are practically important.
One emperical relation

$$N(\mathrm{H}_2) = 3 \times 10^{20} \int T_{b,\nu}(\mathrm{CO}) du [\mathrm{cm}^{-2}] \tag{16}$$

where $T_{b,\nu}$: brightness temperature $I_\nu =: \frac{2\pi T_{b,\nu}}{\lambda^2}$ (Rayleigh-Jeans limit).

Note that this relation tends to have large scatter which depends on C/H ratio, cloud temperature, mass, size ...

8.4 Isotope

Rotational spectra of diatomic molecules can be used to determine **isotopic abundance ratios**.
Considering $^{12}\mathrm{C} \to {}^{13}\mathrm{C}$

- In atoms: $m_e \ll m_{\text{nucleus}}$ and energy levels slightly shift ($E_n = -R/n^2, R \propto \mu \sim m_e$).
- In molecules: μ changes by significant amount and the molecular lines therefore occur at significantly different wavelengths.
- e.g. the lowest rotational transition— $^{12}\mathrm{C}^{16}\mathrm{O} : \lambda 2.60\mathrm{mm}$, $^{13}\mathrm{C}^{16}\mathrm{O} : \lambda 2.48\mathrm{mm}$.

Problems

- Optical depth: low J lines are optical thick and becomes thermal, which is not directly related to the amount of CO. So, $^{12}\mathrm{C}/^{13}\mathrm{C} \neq I(^{12}\mathrm{C})/I(^{13}\mathrm{C})$.
- Chemical fractionation: chemical reaction-rate coefficients differ depending on the nuclear mass.